IMPROVEMENT OF THE IN-PLANE CRUSHING RESPONSE OF CFRP SANDWICH PANELS BY THROUGH-THICKNESS REINFORCEMENTS

L.G. Blok[12*], J. Kratz[1], D. Lukaszewicz[3], S. Hesse[3], C. Kassapoglou[2], C. Ward[1]

[1] ACCIS, University of Bristol, Queen's Building, University Walk, BS8 1TR, Bristol, United Kingdom
* Email: lourens.blok@bristol.ac.uk
[2] Faculty of Aerospace Engineering, Delft University of Technology, Kluyverweg 1, 2629 HS Delft, The Netherlands
[3] BMW Group, Department, Research and Innovation Centre, Knorrstrasse 147, 80788 Munich, Germany

Keywords: composite, energy absorption, sandwich, automotive, dynamic, crushing

Abstract
Fibre reinforced plastic (FRP) composite materials can provide superior specific energy absorption performance over conventional metallic structures. However, they crush in a more unstable manner than their metallic counterparts. FRP sandwich structures may provide a stable crushing mechanism for fibre reinforced materials, as a foam core can support the facesheet laminates during crushing. Previous studies showed that improving the facesheet/core interface is a successful strategy to enhance the crushing response, resulting in a higher energy absorption and more stable crushing front. In this work, an improvement of the in-plane crushing response of sandwich structures is obtained using through-thickness reinforcement in the form of Kevlar tufts. Eight different sandwich configurations (four lay-ups and two foam core types) were compared in dynamic crushing. A drop-tower test rig was used which allowed facesheet debonding and high-speed camera footage was used to analyse the crushing morphology. The through-thickness reinforcement resulted in more localized and stable fracture of the facesheets. This improved the specific energy absorption (SEA) and the crush force efficiency (CFE), showing an average increase from 11.5 kJ/kg to 20.5 kJ/kg and from 0.22 to 0.55, respectively.

1. Introduction

Fibre reinforced composite materials are gaining interest from car manufacturers. They can provide superior energy absorption performance over conventional metallic structures compared on weight basis [1]. The use of composite materials as energy absorbers, however, is still limited as they crush in a more unstable manner than their metallic counterparts [2]. In a real-world crash situation, load scenarios are not well defined and this provides a challenge to designing energy dissipating structures using composite beams and profiles alone [3]. Composite sandwich structures may provide a stable crushing mechanism for fibre reinforced materials. This potentially opens up new load paths for energy absorption, which could not be used before in the design of vehicles.

Typical fibre reinforced plastic (FRP) composite materials crush in a brittle manner, which can result in unstable catastrophic failure but also in a stable progressive end crushing mode. Progressive crushing is characterized by a localized zone of micro fracturing of the composite material consisting of splaying/lamina bending and fragmentation/fibre fracture [1] [4], [5]. Several studies investigated the change in energy absorption of FRP crush tubes using interlaminar toughening techniques [6], surface treatments [7], different matrix properties [8], [9] and different fibre orientations [10]. It can be concluded that the better the interlaminar properties are, the less splaying/lamina bending occurs and the higher the resulting energy absorption becomes.

Multiple studies have been performed related to impacts on sandwich structures, but they have mainly been focused on out-of-plane impacts [10], [11]. The in-plane (or edgewise) crushing of sandwich structures has received less attention. Mamalis et al. [12] reported three different collapse modes; unstable sandwich column buckling (Mode 1); unstable sandwich disintegration by facesheet/core disbonding (Mode 2); and progressive end crushing of the sandwich (Mode 3). It was found that the mechanical properties of the core have a large effect on the type of failure mode. Velecela et al. [13] also investigated the crushing of FRP-foam core sandwiches and came to similar conclusions.

A foam core may stabilize the crushing of the facesheet, but another interface is added which can fail and result in unstable collapse. Stapleton and Adams [14] investigated the effect of crush initiators to promote stable crushing of sandwiches. More recently, they reported on structural enhancements (end-

Excerpt from ISBN 978-3-00-053387-7

bevel, stitching and core webbing) to improve the energy absorption [15]. Their findings suggest that stable sandwich crushing may be realized by improving the facesheet/core interface.
To successfully implement the superior energy absorption of composites, a stable and predictable crushing platform is required. In this work, an improvement in crushing response is obtained by through-thickness reinforcements of Kevlar tufts in a 6x6mm rectangular pattern. These tufts strengthen the interface between the facesheet and the core and prevent premature facesheet separation [16]. Dynamic edgewise compression tests were carried out on eight different sandwich configurations. A customized drop-tower test-rig was used which allowed facesheet/core failure and tracking of the crushing front with a high speed camera. The crushing behaviour of eight sandwich systems were compared which leads to a better understanding of the failure progression.

2. Methodology

2.1. Test fixture

Different sandwich systems were tested under dynamic in-plane crushing using a special test rig [11]. Most studies on in-plane crushing of sandwich panels used a fixed specimen and a moving impactor. In this study, a drop-tower rig is used and the specimen is mounted below a drop-hammer as shown in Figure 1. The mass of the drop hammer can be changed to change the impact energy. The specimen freely falls into four alignment guides. A detail of the crush plate and guides in shown in Figure 2.

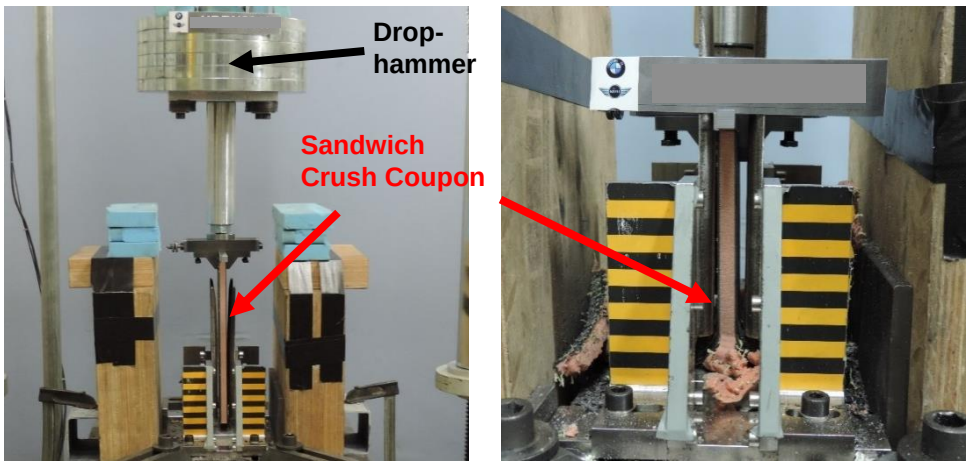

Figure 1. Test set-up showing sandwich crush coupon before and after crushing in test fixture

The advantage of the test set-up used here is that the specimen is not completely supported over its length. This would suppress interface failure between the core and facesheet, as is often observed for sandwiches under edgewise compression. Moreover, it allows to record the crush front using a high speed camera.

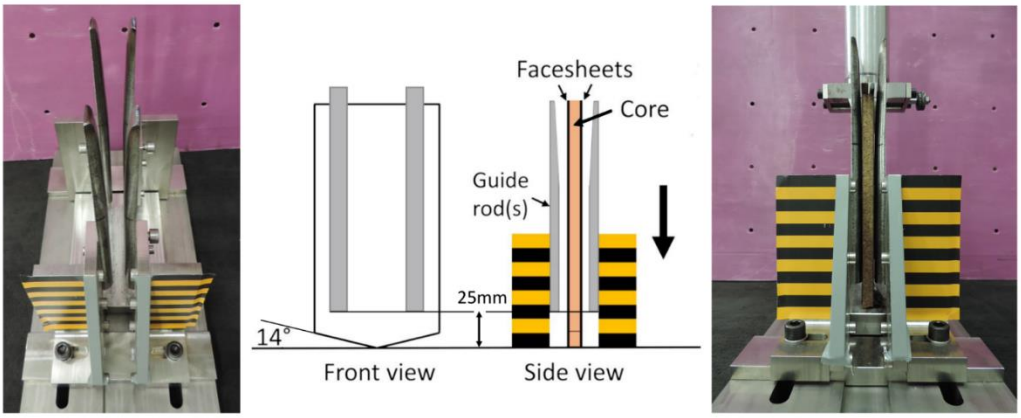

Figure 2. Detail of test fixture showing sandwich specimen and four alignment guide rods and impact plate

Excerpt from ISBN 978-3-00-053387-7

2.2. Test materials

The crush coupon dimensions for the static tests and dynamic tests are shown in Figure 3. Static tests were carried out for initial screening of the sandwich panels, which allowed to predict the energy absorption for the dynamic tests. The crush coupons for the static tests were smaller (70x100mm) than the dynamic coupons (300x120mm). Both coupons included a 14° bevel as shown in Figure 3 to promote stable progressive crushing as Velecela *et al.* [12] determined.

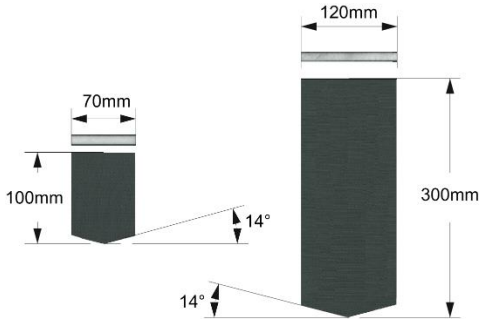

Figure 3. Dimensions of the crush coupons for static (left) and dynamic (right) tests

Sandwich specimens were manufactured using two types of foam; *Rohacell 110 IG-F* polymethacrylimid *(*PMI*)* foam and *Airex C70.90* polyvinylchlorid (PVC) foam (see Table 1 for mechanical properties). The facesheets laminates were made from carbon Non-Crimp Fabrics (NCF). Hand lay-up was used to build the sandwich, after which Kevlar threads were inserted through the dry fibres and the core in a 6x6mm rectangular pattern by a robotic arm using the tufting process [13]. A vacuum infusion process was then used, using an Epikote 935 resin system, to obtain the final plates. The samples were waterjet cut from the plates and no further processing steps were carried out. An example of a tufted sandwich is shown in Figure 4.

Four different lay-ups were used for the facesheet skins; $[0/90/0]$, $[0/90/0]_s$, $[-45/0/45]$ and $[-45/0/45]_s$, yielding eight different sandwich configurations shown in Table 2. For each sandwich configuration, three dynamics tests were performed.

Table 1. Mechanical properties polymer foams as supplied by manufacturer [14], [15]

	Airex C70.90	**Rohacell 110 IG-F**
Density [kg/m^3]	100	110
Compressive strength [MPa]	2.0	3.0
Compressive modulus [MPa]	130	160
Shear modulus [MPa]	40	50
Maximum strain [%]	23	3

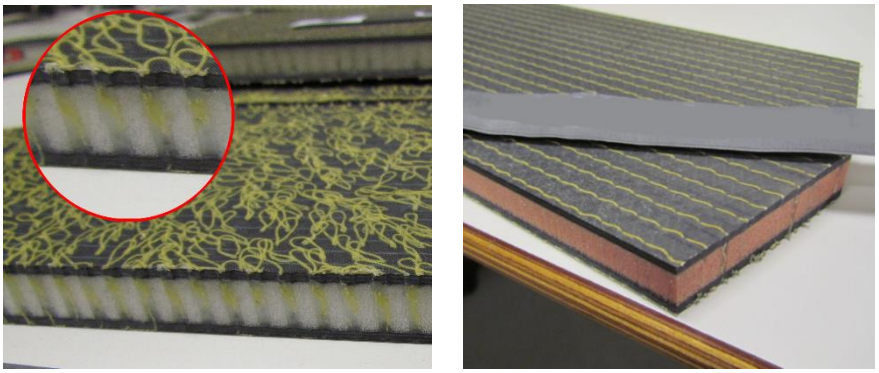

(a) Bottom surface of tufted 110 IG-F sandwich **(b)** Top surface of tufted C70.90 sandwich

Figure 4. Example of tufted sandwich coupon showing both sides

Excerpt from ISBN 978-3-00-053387-7

Table 2. Sandwich configurations for dynamic testing

Facesheet material	Non-Crimp Fabric
Facesheet lay-ups	$[0/90/0]$, $[0/90/0]_s$, $[-45/0/45]$ and $[-45/0/45]_s$
Core materials	Airex C70.90 and Rohacell 110 IG-F
Through-thickness reinforcement	With and without Kevlar tufts.

2.3. Dynamic testing

Dynamic testing was carried out by dropping the sandwich samples under a drop hammer to a crush plate as shown in Figure 1. The drop height was set to have an impact speed v_{imp} of 8.6 m/s. A mass m_{imp} was added to the drop hammer to change the impact energy E_{imp} The impact energy was changed such that a representative amount of crushing occurred for each sandwich system.

Two accelerometers on top of the drop-hammer recorded the acceleration during crushing. The data was then filtered to remove any high frequency oscillation according to the SAE J211 guidelines for impact testing using a CFC 180 filter [16].

The crushing force was determined from the filtered acceleration data a_{acc} through equation (1), where m_{imp} is the mass of the drop hammer. The crushing distance was also determined from the filtered acceleration data, by integrating it twice according to equations (2) and (3), where v_{imp} was the initial velocity, s is the distance travelled, and t is the time. A representative section of crushing was extracted from the force-displacement curve up to a displacement s = 75mm. This was done to obtain a common comparison basis for all sandwich systems.

$$F = m_{imp} a_{acc} \tag{1}$$

$$v(t) = v_{imp} - \int_0^t a_{acc} dt \tag{2}$$

$$s(t) = \int_0^t v dt \tag{3}$$

2.4. Crushing properties

A force-displacement curve for the dynamic test is shown in Figure 6 to illustrate the typical crushing response. Comparison of the crushing performance was done with the following global crushing properties (as indicated in Figure 6). The crushed mass $m_{crushed}$ to determine the specific energy absorption was derived from the crushing distance and the density of the specimen.

- Maximum force during crushing F_{max}
- Average crushing force F_{avg}
- Crush force efficiency CFE (F_{avg}/F_{max})
- Specific energy absorption ($E_{absorbed}/m_{crushed}$)

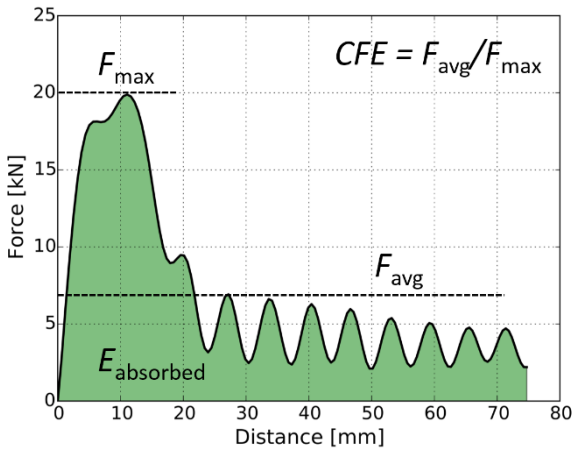

Figure 6. Force-displacement curves of C70.90 [0/90/0] sandwich showing key crushing properties

Excerpt from ISBN 978-3-00-053387-7

3. Results

3.1. Specific energy absorption and crush force efficiency

The specific energy absorption (SEA) of the different sandwich systems under dynamic crushing is shown in Figure 7a. The SEA clearly improved by tufting for all sandwich systems. The average increase in SEA during dynamic crushing for the Rohacell 110 IG-F sandwiches was +110%, and for the Airex C70.90 sandwiches the average increase was 58%.

The SEA of the untufted C70.90 sandwich systems generally exceeded that of the untufted 110 IG-F sandwiches. When the tufted sandwiches are compared, the 110 IG-F sandwiches show a higher SEA than the C70.90 sandwiches. Relatively, the 110 IG-F sandwich systems showed a larger improvement by tufting than similar C70.90 sandwiches.

Figure 7b shows the crush force efficiency. The average improvement during dynamic crushing of the 110 IG-F sandwiches was +100% and +58% for the C70.90 sandwiches. This indicates that the SEA increased by having a higher sustained crushing force compared to the initial peak load.

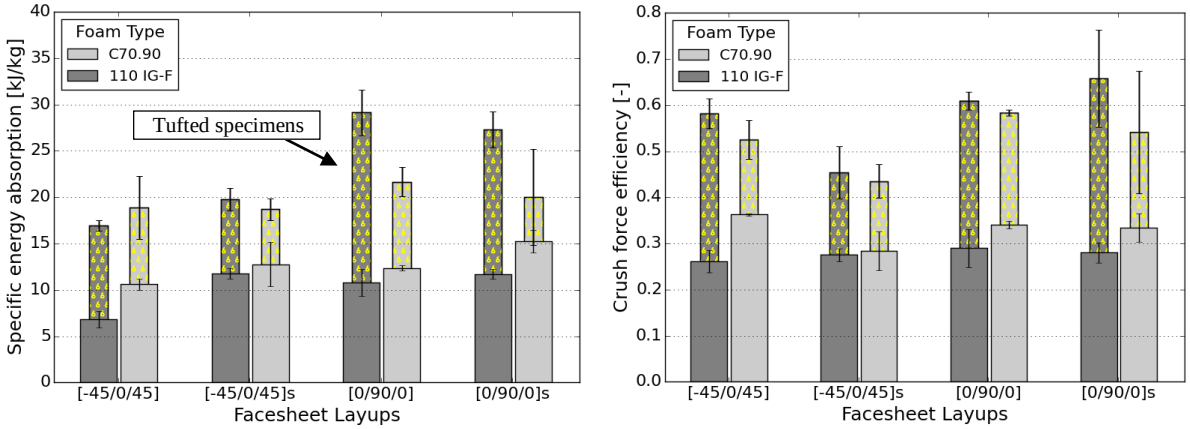

Figure 7: Sandwich crushing properties during dynamic crushing; (a) specific energy absorption and (b) crush force efficiency

3.2. Maximum force and average crushing force

The average crushing force showed a significant improvement by tufting as shown in Figure 8a. This does not take into account the increase in weight for the tufted sandwiches, which explains why the increase in SEA is lower. Similar to the SEA, the 110 IG-F sandwiches show the biggest improvement by tufting compared to the Airex C70.90 sandwiches.

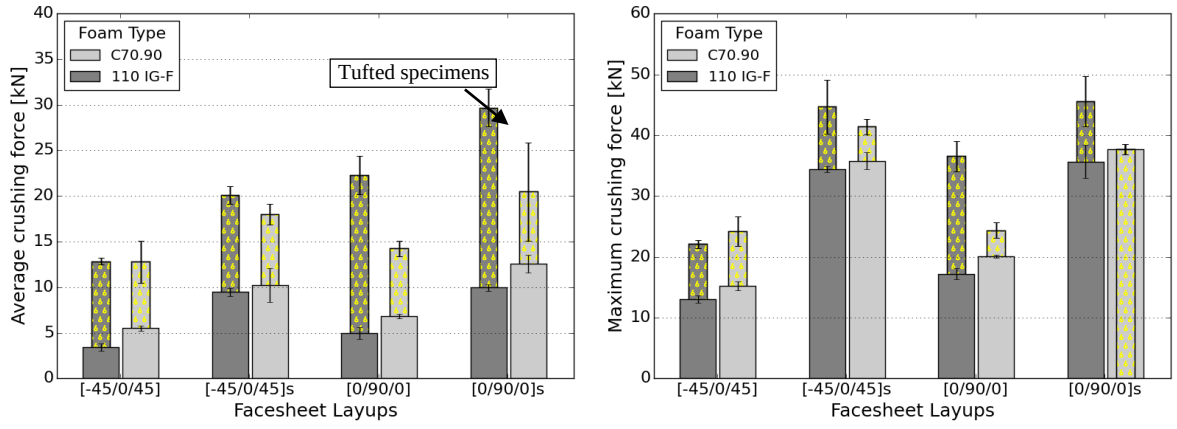

Figure 8: Sandwich crushing properties during dynamic crushing; (a) average crushing force and (b) maximum crushing force

Excerpt from ISBN 978-3-00-053387-7

Figure 8b shows a comparison of the maximum crushing force. The through-thickness reinforcement generally does increase the maximum force, which indicates it is related to initial failure of the facesheet-core interface. For the C70.90 $[0/90/0]_s$ sandwich system, a small decrease in maximum force is recorded. This sandwich system has relatively stiff facesheets and a stabilizing foam core. The 110 IG-F [0/90/0] sandwich systems have thinner facesheets and the 110 IG-F provides less support during crushing. They show the highest increase in maximum force.

3.3. Crushing morphology and force-displacement graphs

The crushing morphology and force-displacement graphs of the 110 IG-F [0/90/0] and C70.90 [0/90/0] sandwiches are shown in Figure 9 and 10. Facesheet-core interfacial failure for the untufted 110 IG-F sandwich is clearly visible from the start of crushing (arrows A,B and C), and remained present throughout crushing. The tufted 110 IG-F specimen shows that the facesheets remained attached to the core and bent through a small radius (arrows D and E) before the fracture processes start.

The failure of the untufted C70.90 [0/90/0] specimen was dictated by delaminations (arrows F and G) in the facesheets which subsequently bent (arrow H), with little fracture of the facesheet or facesheet-core interfacial failure. Instead, core debris built up on the crush plate. For the tufted C70.90 specimens, no delaminations in the facesheet occurred. Although some facesheet-core interface failure still occurred (arrow I), clearly more facesheet fracture (arrow J) was present.

The untufted C70.90 [0/90/0] specimens had a higher energy absorption than the 110 IG-F [0/90/0] specimens. The C70.90 specimens showed delaminations in the facesheet and bending of the facesheet, while the 110 IG-F specimens showed failure of the facesheet-core interface and bending of the facesheet.

For the tufted specimens, fracture of the facesheets was dominant for both the C70.90 specimens and the 110 IG-F specimens. The tufted 110 IG-F specimen, however, showed more fracture and fragmenting of the foam core (arrow K) compared to tufted C70.90 specimen.

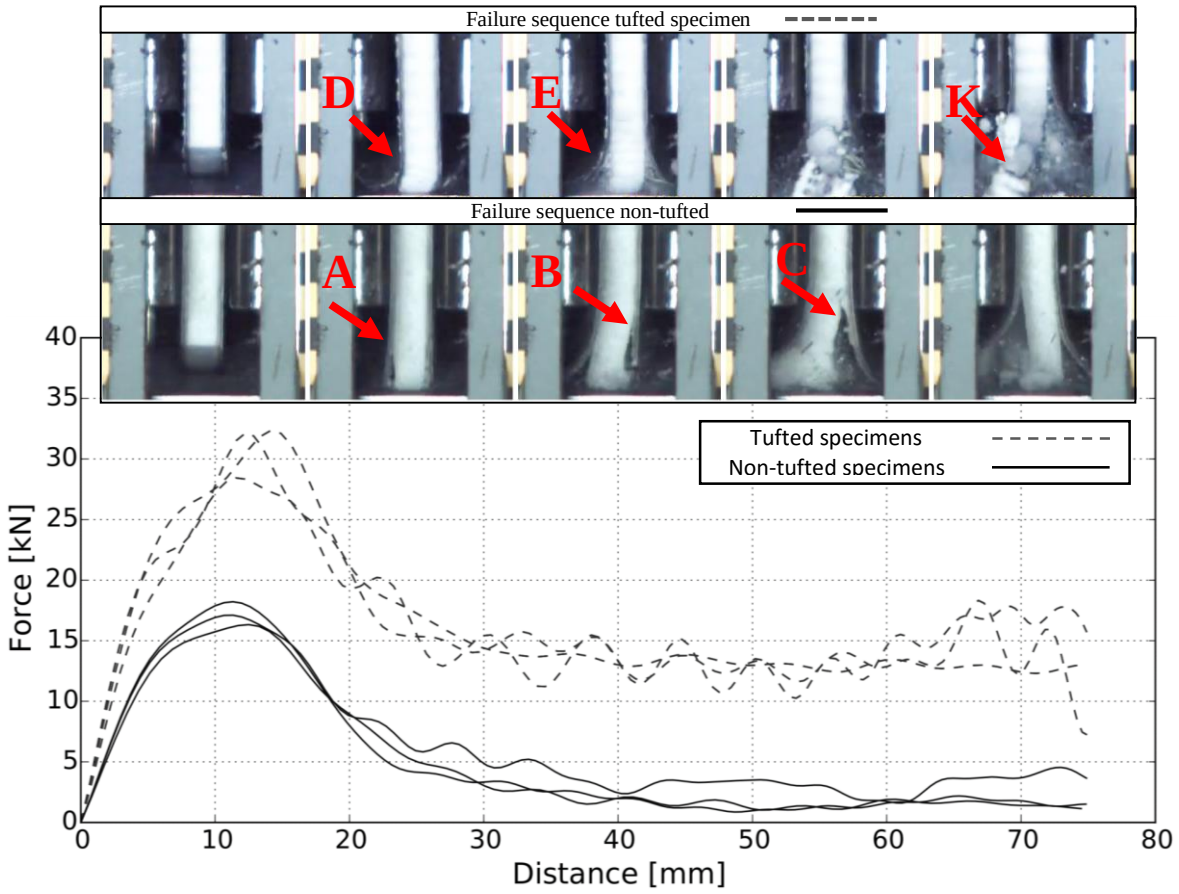

Figure 9. Comparison of force-displacement curves of Rohacell 110 IG-F [0/90/0] sandwiches (3x tufted & 3x non-tufted), with typical failure sequence

Excerpt from ISBN 978-3-00-053387-7

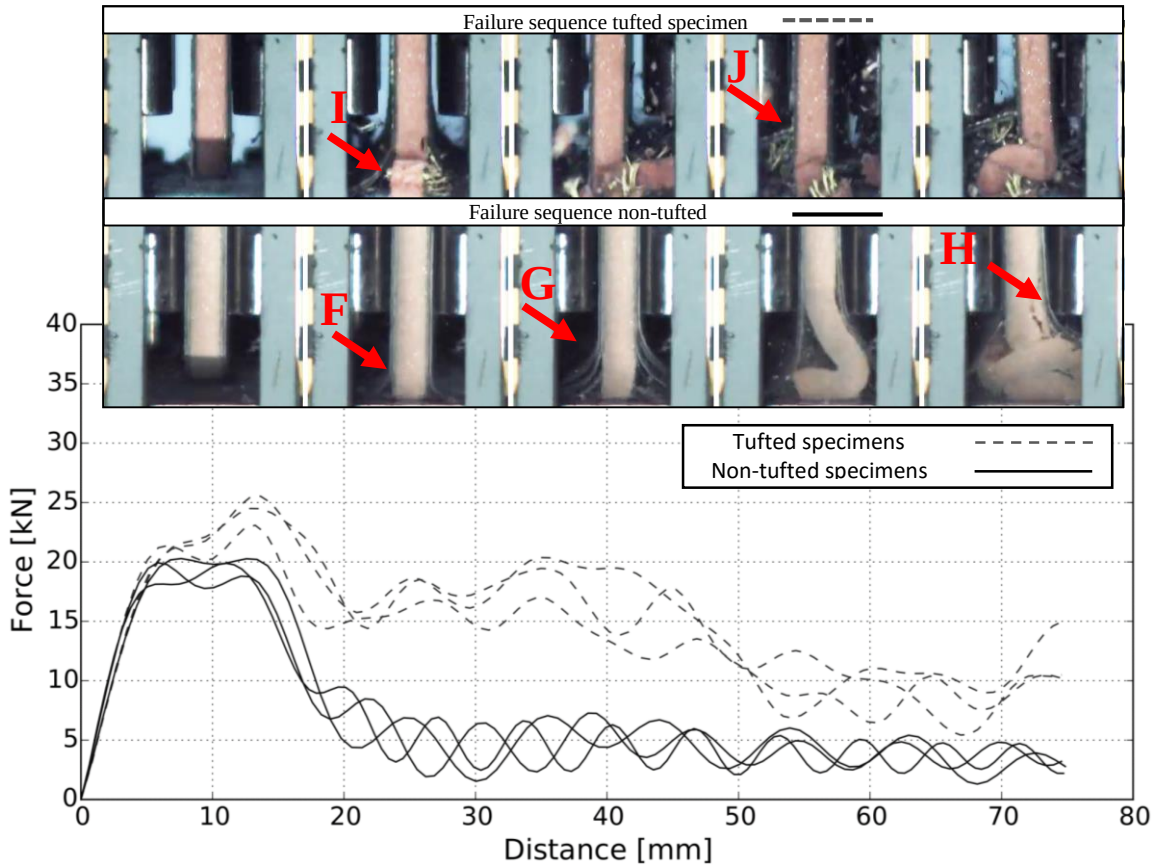

Figure 10. Comparison of force-displacement curves of Airex C70.90 [0/90/0] sandwiches (3x tufted and 3x non-tufted) with typical failure sequence

3. Discussion

The results obtained using the drop-tower test set-up are comparable to those first reported by Mamalis *et al.* [17], where a more ductile foam core better stabilizes the facesheets during crushing. This was shown by comparing the crushing properties of the untufted C70.90 and 110 IG-F sandwiches, as well as a higher increase by tufting in SEA and CFE for the brittle 110 IG-F foam core.

The average crushing force of the untufted sandwiches during dynamic crushing seems to double for the facesheets with double the thickness, while the increase in SEA is less. For the tufted sandwiches, there was no significant improvement in SEA by increasing the facesheet thickness. This indicates that the SEA is driven by crushing of the FRP facesheets, and that there is an upper limit where crushing is at its optimum. An interesting follow-up study for this would be to investigate the influence of the tufting pattern.

High-speed camera footage allowed to identify the failure sequence of sandwiches during progressive crushing. The failure sequence of untufted sandwiches consisted of a repetitive cycle of facesheet/core interface failure, followed by bending of the facesheet and (fibre) fracture the facesheet. For the C70.90 core, delaminations in the facesheets were dominant which reduced the bending stiffness and the amount of fracture in the facesheet. The 110 IG-F core showed large areas of facesheet/core interface failure, which indicates poor performance in supporting the facesheet during crushing as seen before.

The effect of tufting may therefore be twofold; it improves the facesheet/core interface and it prevents premature delaminations in the facesheet itself. All tufted sandwiches showed more localized crushing. The 110 IG-F sandwiches showed slightly higher SEA, which may be attributed to the higher mechanical properties. In this study, only the total energy absorption of the sandwich was looked at. Other research is being done on identifying failure mechanisms in the tufts [18]. Identifying the individual contributions of the core, facesheets and fracture of the Kevlar thread tufts may help understand the crushing process better.

Excerpt from ISBN 978-3-00-053387-7

3. Conclusions

An improvement in both specific energy absorption and crush force efficiency of CFRP/foam core sandwich panels was obtained by adding through-thickness reinforcement in the form of Kevlar tufts. The SEA increased on average by 78%. Moreover, the average crush force efficiency (F_{avg}/F_{max}) increased from 0.24 to 0.55.

High-speed video data showed the differences between crushing morphology of the tufted and non-tufted specimens. For the non-tufted sandwiches, failure was dominated by facesheet-core debonding and delaminations in the facesheets. This inhibited fracture of the actual carbon fibres, which is the main energy absorption mechanism. The tufted specimens showed more localized and stable fracture of the facesheets, leading to better crushing performance.

Concluding, through-thickness reinforcements showed the ability to stabilize and tailor the crushing response of fibre reinforced sandwiches. This may be used to open up new load-paths in crash structures and thereby increasing robustness in a larger variety of load cases.

Acknowledgements

The author would like to acknowledge support for disseminating this work from The Institute of Materials, Minerals and Mining (IOM3) and the EPSRC Centre for Doctoral Training in Advanced Composites for Innovation and Science, and thank Mr. Greissl and Mr. Palmer for conducting the tests.

References

[1] J. J. Carruthers, “Energy absorption capability and crashworthiness of composite material structures: a review,” *Appl. Mech. Rev.*, vol. 51, no. 10, pp. 635–649, 1998.
[2] W. Johnson, “The elements of crashworthiness: scope and actuality,” *Proc. Inst. Mech. Eng. Part D J. Automob. Eng.*, vol. 204, no. 4, pp. 255–273, 1990.
[3] D. H.-J. A. Lukaszewicz, “Automotive Composite Structures for Crashworthiness,” in *Advanced Composite Materials for Automotive Applications*, John Wiley & Sons Ltd, 2013, pp. 99–127.
[4] D. Hull, “A unified approach to progressive crushing of fibre-reinforced composite tubes,” *Compos. Sci. Technol.*, vol. 40, no. 4, pp. 377–421, Jan. 1991.
[5] G. L. Farley and R. M. Jones, “Crushing Characteristics of Continuous Fiber-Reinforced Composite Tubes,” *J. Compos. Mater.*, vol. 26, no. 1, pp. 37–50, Jan. 1992.
[6] N. A. Warrior, T. A. Turner, F. Robitaille, and C. D. Rudd, “The effect of interlaminar toughening strategies on the energy absorption of composite tubes,” *Compos. Part A Appl. Sci. Manuf.*, vol. 35, no. 4, pp. 431–437, Apr. 2004.
[7] H. Hamada, S. Ramakrishna, M. Nakamura, Z. Maekawa, and D. Hull, “Progressive crushing behaviour of glass/epoxy composite tubes with different surface treatment,” *Compos. Interfaces*, vol. 2, no. 2, pp. 127–142, 1994.
[8] P. H. Thornton and R. A. Jeryant, “Crash energy management in composite automotive structures,” *Int. J. Impact Eng.*, vol. 7, no. 2, pp. 167–180, 1988.
[9] W. H. Tao, R. E. Robertson, and P. H. Thornton, “Effects of material properties and crush conditions on the crush energy absorption of fiber composite rods,” *Compos. Sci. Technol.*, vol. 47, no. 4, pp. 405–418, Jan. 1993.
[10] G. L. Farley, “Energy Absorption of Composite Materials,” *J. Compos. Mater.*, vol. 17, no. 3, pp. 267–279, Jan. 1983.
[11] D. Lukaszewicz, S. Engel, and C. Boegle, “Testing of sandwich structures with CFRP skins in edgewise compression,” in *International Conference on Composite Materials-ICCM19*, 2013.
[12] O. Velecela and C. Soutis, “Prediction of crushing morphology of GRP composite sandwich panels under edgewise compression,” *Compos. Part B Eng.*, vol. 38, no. 7–8, pp. 914–923, Oct. 2007.
[13] G. Dell’Anno, D. D. Cartié, I. K. Partridge, and A. Rezai, “Exploring mechanical property balance in tufted carbon fabric/epoxy composites,” *Compos. Part A Appl. Sci. Manuf.*, vol. 38, no. 11, pp. 2366–2373, 2007.
[14] 3A Composites, “Airex C70 Data sheet,” vol. 2011, 2011.
[15] Evonik Industries AG, “Rohacell IG/IG-F Technical Information,” 2014.
[16] Society of Automotive Engineers, “Instrumentation for Impact Tests - Part 1 - Electronic Instrumentation - SAE J211/1.” pp. 34.344 – 34.35, 1995.
[17] A. G. Mamalis, D. E. Manolakos, M. B. Ioannidis, and D. P. Papapostolou, “On the crushing response of composite sandwich panels subjected to edgewise compression: experimental,” *Compos. Struct.*, vol. 71, no. 2, pp. 246–257, Nov. 2005.
[18] J. W. Hartley, G. Tse, J. Kratz, C. Ward, and I. Partride, “Column Interaction In Tufted Sandwich Structures Under Edgewise Loading,” in *ECCM17 - 17th European Conference on Composite Materials*, 2016.

Excerpt from ISBN 978-3-00-053387-7